Pergamon International Journal of Machine Tools & Manufacture 41 (2001) 1721–1734

INTERNATIONAL JOURNAL OF MACHINE TOOLS & MANUFACTURE DESIGN, RESEARCH AND APPLICATION

Forecast of shear spinning force and surface roughness of spun cones by employing regression analysis

M.D. Chen [a], R.Q. Hsu [a,*], K.H. Fuh [b]

[a] *Department of Mechanical Engineering, National Chiao Tung University, 1001 Ta-Hsueh Road, 300 Hsinchu, Taiwan*

[b] *Department of Mechanical and Marine Engineering, National Taiwan Ocean University, Taiwan*

Received 23 August 2000; received in revised form 7 March 2001; accepted 16 March 2001

Abstract

A series of shear spinning experiments has been performed to produce axi-symmetric cones from blank sheet. The experiments investigated influences of roller nose radius, mandrel revolution and roller feed on the spinning force and the inside/outside surface roughness of spun cone. Statistical analysis was adopted to construct the regression equations governing these parameters. Independent experiments verified the findings. It was discovered that the established regression equations possess a significant degree of reliability. © 2001 Elsevier Science Ltd. All rights reserved.

Keywords: Shear spinning; Shear force; Response surface method; Regression analysis; Over-roll

1. Introduction

Metal spinning methods can be classified as shear spinning (shear forming), contour spinning and flow turning. In shear spinning, a plate or blank sheet is mounted on a revolving mandrel, while a roller presses on the blank to form a cone shaped product. During the spinning process, a reduction of the blank thickness (shearing) occurs along the longitudinal axis of the cone. Shear spinning product shapes include cylindrical tubes, concave or convex cones and hollow or stepped tubes. This work focuses on the spinning of cone shaped product. Many factors affect the shear spinning process, including the material characteristics of blank, blank thickness, roller nose radius, cone angle, roller feed and mandrel revolution. Combinations of these variables signifi-

* Corresponding author. Tel.: +886 35 712121; fax: +866 35 720634.
E-mail address: rqhsu@cc.nctu.edu.tw (R.Q. Hsu).

PII: S0890-6955(01)00039-6

Nomenclature

t_0; x_1	original thickness of blank (mm)
ρ_R; x_2	roller nose radius (mm)
N; x_3	mandrel revolution (rev/min)
f; x_4	roller feed (mm/rev)
k	number of variable parameters
α	half apex angle of mandrel (degree)
ψ	roller position angle (degree)
Fq	normal force Newton (N)
Fp	feeding force Newton (N)
Ft	tangential force Newton (N)
Ro	outer surface roughness of part ($\mu m=10^{-3}$ mm)
Ri	inner surface roughness of part ($\mu m=10^{-3}$ mm)

cantly affect both the force required for spinning and final product quality, especially the cone surface roughness.

In cone spinning studies, Kobayashi [1,2] and Kalpakcioglu [3,4] published several pioneering works. These studies presented both the flow patterns and the spinning forces and derived an analytical prediction of the spinning forces.

Initially, Siebel [5] offered experimental graphs of the maximum radial and axial spinning forces. That investigation then calculated the corresponding tangential forces from the power consumption. However, the power consumption was computed by neglecting both the redundant power and friction losses. Feola [6] experimentally measured the radial spinning force and feed forces of flanged cone products. Feola also discussed the effects of the process variables on the buckling and bending of the flange.

More recently, Held [7] discovered that copper cone product performances applied in high velocity jet depends upon the inner and exterior surface roughness as well as the type of manufacturing process. However, the above studies despite their contributions, were limited to a discussion of one particular variable's effect on only the spinning force. That is, the combined parameter influences on both the spinning force and the surface roughness of the spinning product failed to be discussed. Therefore, the effects of process variables on the product surface roughness and spinning force must be more closely examined. Thus, in this study, we statistically designate experimental sets, in which the effects of each process parameter and the mutual interactions on both spinning force and cone surface roughness are investigated simultaneously. Although Wang [8] indicated that with high temperature multi-pass spinning processes, surface roughness of the cone shape product was improved, a satisfactory surface roughness has been achieved in the present experiment with a single-pass spinning process. Finally, the experiments cited in this study provide sufficient data for a statistical analysis, which in turn results in regression equations for surface roughness and forces.

2. Parameter arrangements and experimental procedure

2.1. Response surface method and parameter arrangements

Fig. 1 illustrates the analysis procedure applied in this study. Since several factors affect the spinning process, the experiments are statistically arranged to avoid the negligence of any particular variable. The Response Surface Method (RSM) [9] was chosen for this purpose.

RSM adopts both mathematical and statistical techniques beneficial for investigating phenom-

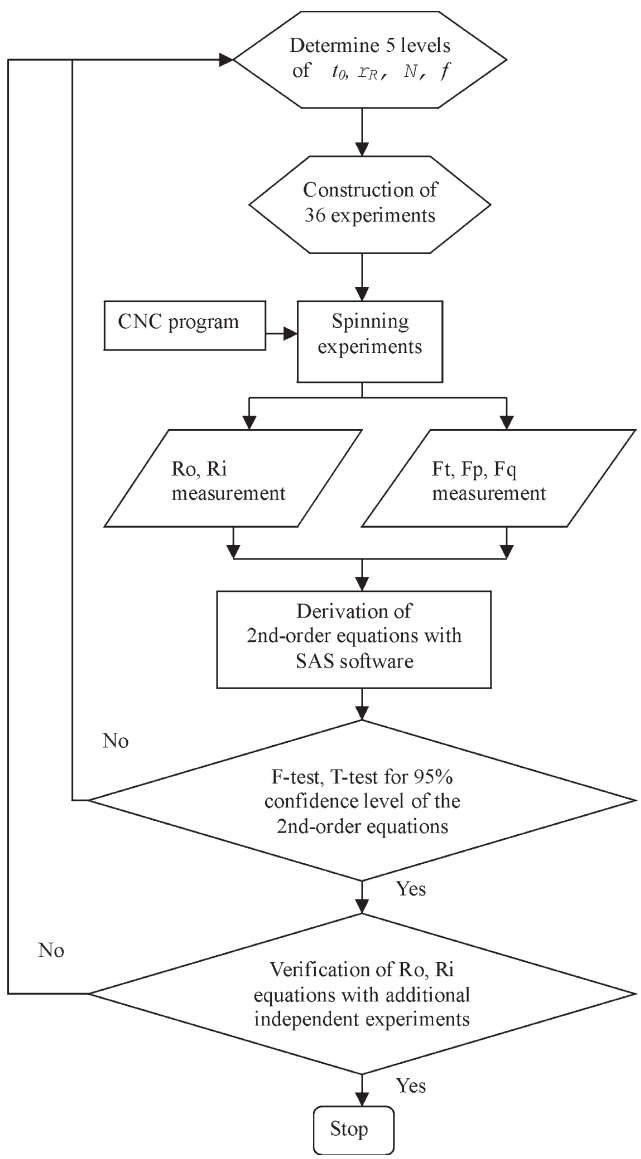

Fig. 1. Analysis procedure.

ena with several independent variables. RSM attempts to analyze the influence of these independent variables on a specific dependent variable (response). Initially the independent variables of a problem are symbolized by $x_1, x_2,\ldots, x_k$. These variables are presumed to be continuous and can be controlled with negligible error in the experiments. The response (e.g., Y) is postulated to be a random variable. For example, to find the blank thickness (x_1) and roller rose radius (x_2) that minimize the outer surface roughness (Y) yield of a spun cone, the detected response Y as a function of the levels of x_1 and x_2 is written as:

$$Y=f(x_1, x_2)+\varepsilon \tag{2.1}$$

where ε represents an error component. Fig. 2 demonstrates that if the expected response is denoted by $E(Y-\varepsilon)$=Ro, then the surface represented by Ro=$f(x_1, x_2)$ is termed as the response surface. In most RSM problems, the relationship between the response and the independent variables is unknown. Therefore, the primary step in RSM is to postulate a suitable approximation for Y and the independent variables set. If the response is a linear function of the independent variables, then first-order equations can be employed, otherwise, higher order equations are applied. For example, the second-order Eqs. (2.2) proposed by Montgomery [10] is often adopted.

$$Y=b_0+\sum_{i=1}^{k} b_i x_i+\sum_{i=1}^{k} b_{ii} x_i^2+\sum_{i}^{k}\sum_{j}^{k} b_{ij(i<j)} x_i x_j+\varepsilon \tag{2.2}$$

$$\frac{\partial Y}{\partial x_i}=\frac{\partial Y}{\partial x_2}=\ldots=\frac{\partial Y}{\partial x_k}=0. \tag{2.3}$$

Polynomials are typically approximated by least square functions. Response surface obtained by the least square function is referred to as the fitted surface. If the fitted surface is sufficiently

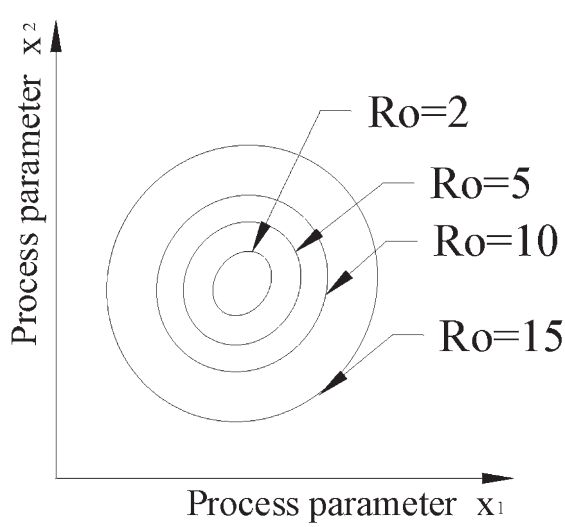

Fig. 2. The response surface.

close to the true response function, then the fitted surface analysis will be a close approximation to the actual system analysis.

In this study, the blank thickness t_0, roller nose radius ρ_R, mandrel revolution N and roller feed f are chosen for the shear spinning process as the independent process parameters, indicated in Eq. (2.2) as x_1, x_2, x_3 and x_4, respectively. Furthermore, the constants b_0, b_i, b_{ii} and b_{ij} are determined by the least square method, while Y is the estimated response for either spinning force (Ft, Fp, Fq) or the surface roughness (Ro, Ri) of the product. Once the experimental results are derived, the coefficients of the above functions can be calculated, then the variance analysis is performed with Statistics Analysis System (SAS/STAT) software to determine the weight of the parameters (T-test). Then to verify the adequacy for the proposed equation, an F-ratio test is conducted. Functions thus determined are named regression equations, whereas the mathematical procedures are dubbed regression analysis.

If each experimental parameter is adequately investigated, then a response surface becomes the most efficient match. Each experimental parameter must contain at least three levels to construct a second order equation model. In this investigation, four parameters (x_1, x_2, x_3, x_4) each with five levels (0, ±1, ±2) are selected for experiments as shown in Table 1.

2.2. Experimental procedure

The shear spinning parameters scheduled from RSM to formulate statistical regression equations, the spinning force and surface roughness data are compiled and then fed into the SAS/STAT program.

Fig. 3 is a schematic diagram of the shear spinning device. It is constructed from a CNC lathe. Spindle power rate is 15 HP, the longitudinal (Z axis) and the latitude (X axis) output are 5 HP and 3 HP, respectively. The spindle rotates from 100 to 1500 rpm. Forming roller can feed from 0 to 2000 mm/min in X axis and 0 to 3000 mm/min in Z axis. A fixture was designed to let the clamping end move concurrently with the forming roller in the axial direction. The CNC controller adjusts the mandrel revolutions and roller feeds. Once the mandrel contour and work-piece dimensions were determined, the shear spinning process was conducted via a computer program.

Fig. 4 presents the mandrel dimensions. It is comprised of precisely turned and polished Cr–

Table 1
Variation of shear spinning parameters

Shear spinning parameters	Symbols	Levels				
		−2	−1	0	+1	+2
Blank thickness t_O (mm)	x_1	1.5	2.59	4.11	6.0	7.0
Roller nose radius (mm)	x_2	2.5	4.0	4.8	5.5	7.1
ρ_R Mandrel revolution N (rev/min)	x_3	20	40	60	80	90
Roller feed f (mm/rev)	x_4	0.1	0.13	0.16	0.18	0.20

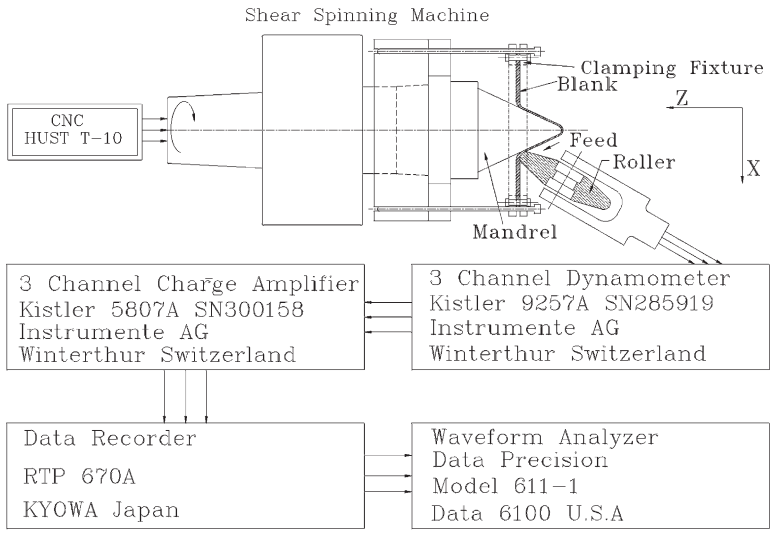

Fig. 3. Experimental device.

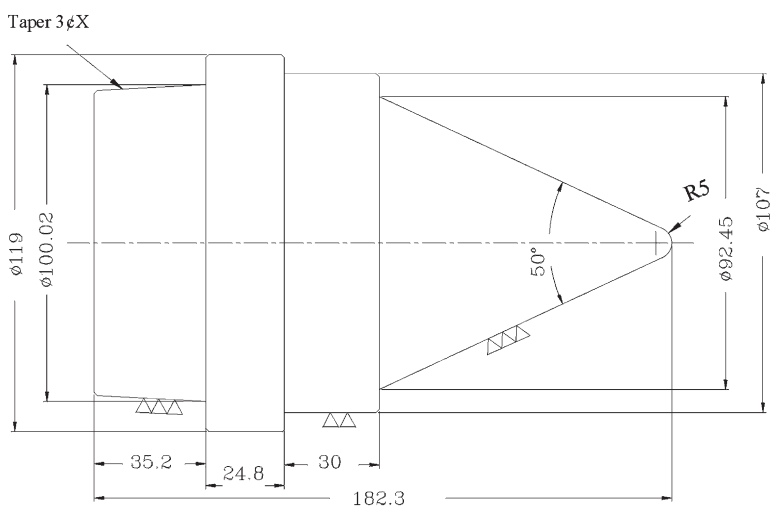

Fig. 4. Mandrel dimensions.

Mo alloys (SAE 4130), then heat-treated to a hardness of Rc 60-63. Cone angle at the tip of the mandrel was 50° and the nose radius equaled 5 mm. Fig. 5 depicts the four types of forming rollers generally employed in industrial practice. Type (d) was adopted in the experiment. It also displays the detailed dimensions of these rollers. The rollers are comprised of the same Cr–Mo alloys (SAE 4130) as the mandrel. Its surface was heat-treated to a hardness of Rc 60-63. The blank material used in these experiments was an 1100-O Aluminum, with five distinct blank sheet thicknesses (1.50, 2.59, 4.11, 6.0 and 7.0 mm). Fig. 6 demonstrates blank layout dimensions.

To measure the force, a three-channel dynamometer (Kistler 9257A) was selected along with a three-channel charge amplifier (Kistler 5807A) amplified the force output signals. For the con-

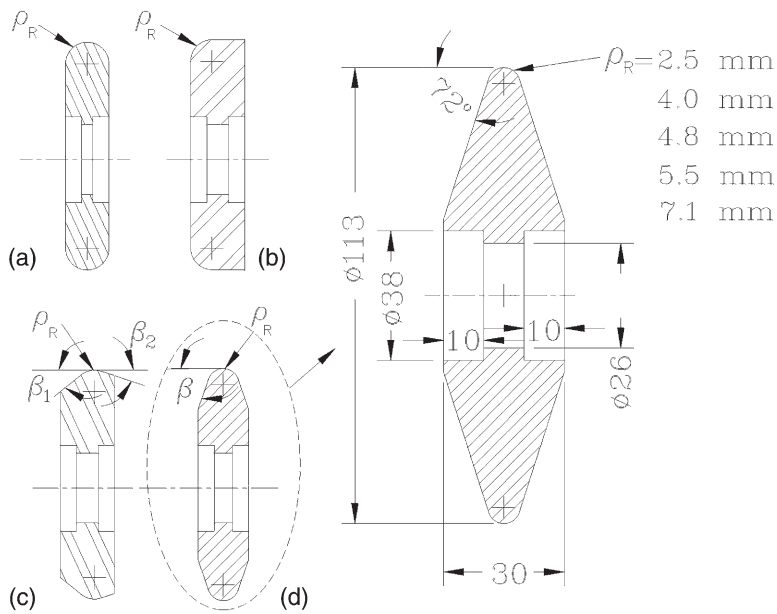

Fig. 5. Spinning rollers.

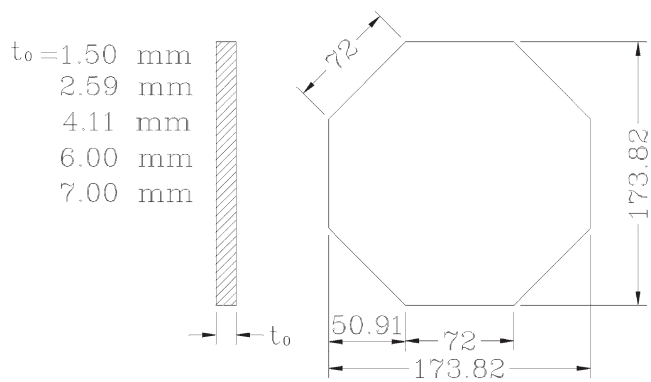

Fig. 6. Blank dimensions.

venience of analysis, a data recorder (KYOWA RTP 670A) was connected to the amplifier. Then, a waveform analyzer (Data Precision Model 611-1) carefully analyzed the recorded data.

A surface roughness measuring instrument (Talysurf 6, Tayler–Hobson) recorded the inside and outside surface roughness of the spun cones.

Interference between roller and blank flange and clamping fixture must be avoided during spinning process. Fig. 7 illustrates the roller contact angle ψ, which is the angle formed by the roller axis and mandrel axis, fixed at 60° throughout the operation. Additionally, 0.5 mm over-roll (thinning) of the blank thickness was applied to all the spinning processes.

Table 2 presents the shear spinning parameter combinations of 36 experiments scheduled from

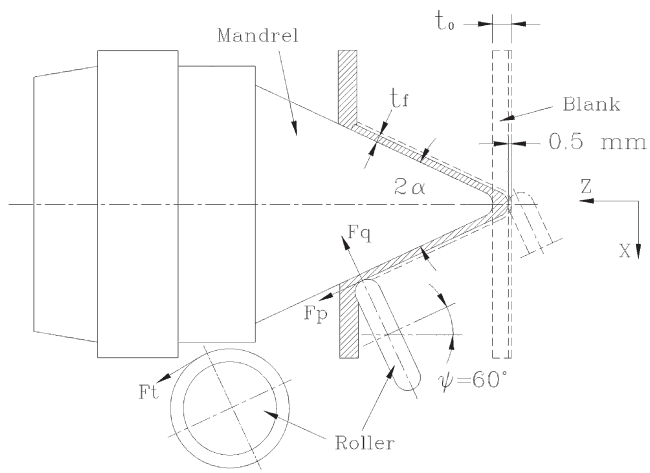

Fig. 7. Three shear force components of shear spining.

RSM. It also depicts the normal force (Fq), feeding force (Fp), tangential force (Ft) and the surface roughness (Ri, Ro) measured in these experiments.

3. Results and discussion

3.1. Results

Experimental results listed in Table 2 were fed into a SAS software package to establish a set of regression equations. These equations demonstrate the correlation among the inner, outer surface roughness, spinning force and the process parameters.

The equation for inner surface roughness Ri is derived as follows:

$$\mathrm{Ri}=4.01+0.83t_0-53.47f+0.20t_0^2-0.45t_0\rho_R+10.15\rho_R f. \tag{3.1}$$

Here, mandrel revolution N does not appear in Eq. (3.1), because its weight was negligible from analysis. The F-value of Eq. (3.1) is 16.519, which is greater than $F_{0.05}(5,30)=4.5115$. It demonstrates that within a 95% confidence interval, the equation is acceptable.

Similarly, the outer surface roughness (Ro) is derived in the following form:

$$\mathrm{Ro}=-1.15+0.70t_0-0.09\rho_R-0.004N+22.55f-0.06t_0\rho_R+0.001\rho_R N-0.83\rho_R f \tag{3.2}$$
$$-0.08Nf$$

The F-value of the equation is 3.345, which is greater than $F_{0.05}(8,27)=2.856$. Therefore, this prediction equation is acceptable within a 95% confidence level.

The equation for tangential force (Ft) along the cone surface is also derived as follows:

$$\mathrm{Ft}=739.03+1.50t_0-29.34\rho_R-3.24N-6112.49f+4.60t_0^2+4.77\rho_R^2+0.04N^2+21186f^2 \tag{3.3}$$
$$+0.42t_0\rho_R-0.26t_0N+44.39t_0f-0.02\rho_R N-81.87\rho_R f-0.27Nf.$$

Table 2
Spinning parameter combinations and experimental results

	Shear spinning parameters				Experimental measuring results				
	t_0 (mm)	ρ_R (mm)	N (rev/min)	f(mm/rev)	*Ri[a] (μm)	*Ro[a] (μm)	Fq (N)	Fp (N)	Ft (N)
1	2.59	4.0	40	0.13	1.21	1.35	690.2	458.2	160.2
2	2.59	5.5	40	0.13	1.23	1.14	710.2	457.4	192.8
3	6.00	4.0	40	0.13	5.09	2.85	965.4	557.8	324.8
4	6.00	5.5	40	0.13	1.15	2.15	992.2	587.2	341.8
5	2.59	4.0	40	0.18	0.80	1.81	728.2	457.4	184.2
6	2.59	5.5	40	0.18	1.16	1.51	761.2	478.8	209.2
7	6.00	4.0	40	0.18	2.45	3.05	991.6	587.2	332.4
8	6.00	5.5	40	0.18	1.08	2.45	999.4	597.6	353.3
9	2.59	4.0	80	0.18	1.10	1.50	679.4	437.6	202.8
10	2.59	5.5	80	0.18	1.06	1.22	750.6	457.2	222.7
11	6.00	4.0	80	0.18	2.54	2.63	945.4	538.6	333.4
12	6.00	5.5	80	0.18	1.01	2.18	960.4	596.8	362.8
13	2.59	4.0	80	0.13	1.08	1.05	733.2	457.4	210.5
14	2.59	5.5	80	0.13	1.47	1.02	750.6	507.2	225.1
15	6.00	4.0	80	0.13	2.54	2.59	917.0	510.2	298.2
16	6.00	5.5	80	0.13	0.97	1.95	1012.4	558.2	327.3
17	1.50	4.8	60	0.16	1.17	1.54	809.0	410.6	158.3
18	7.00	4.8	60	0.16	4.90	5.66	1058.9	878.2	250.4
19	4.11	2.5	60	0.16	1.01	4.09	968.2	457.1	231.5
20	4.11	7.1	60	0.16	0.84	1.65	980.7	456.9	210.2
21	4.11	4.8	20	0.16	1.07	3.43	987.0	501.5	232.0
22	4.11	4.8	90	0.16	1.01	2.05	1018.3	516.0	203.4
23	4.11	4.8	60	0.10	1.24	2.20	947.8	506.2	231.3
24	4.11	4.8	60	0.20	1.34	4.77	839.0	502.6	231.8
25	4.11	4.8	60	0.16	1.26	2.17	922.0	494.6	221.5
26	4.11	4.8	60	0.16	0.99	2.88	1123.6	506.2	243.5
27	4.11	4.8	60	0.16	1.10	3.37	871.6	494.6	205.1
28	4.11	4.8	60	0.16	1.08	3.38	907.4	520.6	207.3
29	4.11	4.8	60	0.16	0.99	2.19	862.4	514.2	210.9
30	4.11	4.8	60	0.16	1.30	2.51	917.9	509.2	213.7
31	4.11	4.8	60	0.16	1.28	2.75	885.5	505.5	210.0
32	4.11	4.8	60	0.16	1.13	2.19	871.8	510.9	199.2
33	4.11	4.8	60	0.16	1.11	2.32	925.0	510.9	186.9
34	4.11	4.8	60	0.16	1.36	2.59	919.3	520.4	194.5
35	4.11	4.8	60	0.16	0.99	2.62	939.0	506.4	199.4
36	4.11	4.8	60	0.16	1.36	3.25	920.4	511.4	191.8

[a] *Ri, *Ro; ISO ten point height parameter. It is the average height difference between the five highest peaks and the five lowest valleys within the sampling length.

Table 3
Comparison of predicted inner/outer surface roughness with four extra shear spinning experiments

	t_0 (mm)	ρ_R (mm)	N (rev/min)	f (mm/rev)	*Ri (μm)[a]			*Ro (μm)[a]		
					Pre.	Exp.	Error (%)	Pre.	Exp.	Error (%)
1	4.11	4.0	35	0.11	1.99	1.78	10.55	2.19	2.39	9.13
2	4.11	4.0	55	0.11	1.99	1.85	7.04	2.01	1.95	2.99
3	2.59	4.0	35	0.11	1.42	1.28	9.86	1.49	1.50	0.67
4	2.59	4.0	35	0.14	1.04	1.14	9.62	1.98	1.85	6.57

[a] *Ri, *Ro; ten-point roughness.

The F-value of the above equation shows that it is acceptable with a 95% confidence interval, because the F-value is 6.541 which is greater than $F_{0.05}(14,21)=2.378$.

Similarly, the feeding force (Fp) is derived as the following equation:

$$\mathrm{Fp}=94.94-117.09t_0+98.90\rho_R+2.99N+3001.94f+11.74t_0^2-12.10\rho_R^2-0.03N^2 \quad (3.4)$$
$$-10475f^2+4.50t_0\rho_R-0.25t_0N+340.0t_0f+0.48\rho_RN-137.17\rho_Rf-7.61Nf.$$

The F-value of the above equation is 5.123 which is greater than $F_{0.05}(14,21)=2.378$, showing that this equation has a 95% confidence level.

In the same way, the normal force (Fq) is represented as follows:

$$\mathrm{Fq}=-665.92+194.85t_0-18.52\rho_R+3.23N+12742f-12.29t_0^2+4.45\rho_R^2-0.01N^2 \quad (3.5)$$
$$-32801f^2-0.26t_0N-58.89t_0f+0.47\rho_RN-245.05\rho_Rf-24.17Nf.$$

The F-value is 3.915, which is greater than $F_{0.05}(13,22)=2.439$. It depicts that within a 95% confidence level, the equation is acceptable.

To verify the reliability of regression equations stated above, four extra shear spinning experiments with parameter combinations shown in Table 3 were conducted. Fig. 8 presents the spun cones from these independent experiments. Comparison of the predicted data derived from Eqs. (3.1) and (3.2) with the experimental results are listed in Table 3. It was found that the numerical discrepancies for these independent experiments are within 11%. Therefore, results from equations are in agreement with the experiments.

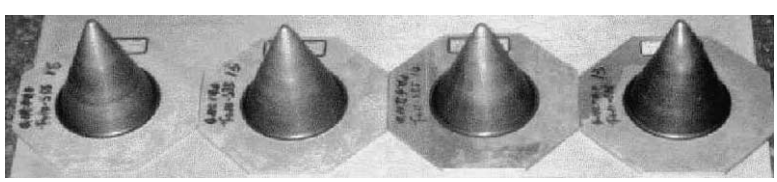

Fig. 8. Spun cones from four extra shear spinning parameters.

4. Discussion

Substituting ρ_R=4.8 mm in Eq. (3.1), the inner surface roughness response of blank thickness and roller feed becomes:

$$\mathrm{Ri}=4.01-1.33t_0+0.2t_0^2-4.75f. \tag{3.6}$$

Fig. 9 depicts the effects of blank thickness and roller feed on inner surface roughness. With fixed roller feed, the inner surface roughness tends to decrease initially with an increasing blank thickness, while the blank thickness reaches 3.0 mm, the inner surface roughness attains to a minimum. Conversely, for blank thickness greater than 3.0 mm, inner surface roughness tends to increase with the blank thickness. This indicates a minimum inner surface roughness exists for a particular blank thickness.

For t_0=4.11 mm and N=60 rev/min, Eq. (3.2) reduces to:

$$\mathrm{Ro}=1.49-0.28\rho_R+17.75f-0.83\rho_R f. \tag{3.7}$$

Fig. 10 displays the effects of the roller nose radius on outer surface roughness at various roller feeds as obtained from Eq. (3.7). The configuration confirms that as the roller nose radius increases, the outer surface roughness decreases in size. Alternatively, with an increasing roller feeds, the outer surface roughness also increases. Therefore, slower roller feeds, when combined with a larger roller nose radius result in an improved outer surface roughness of the spun cone. Since the outer surface of the blank is in direct contact with the roller, a larger roller nose radius implies a larger contact area, thus producing a smoother deformation of the material. While a slower feed can also reduce the material deformation rate, it also improved outer surface roughness.

With a substitution of t_0=4.11 mm and ρ_R=4.8 mm into Eq. (3.3), the following is obtained:

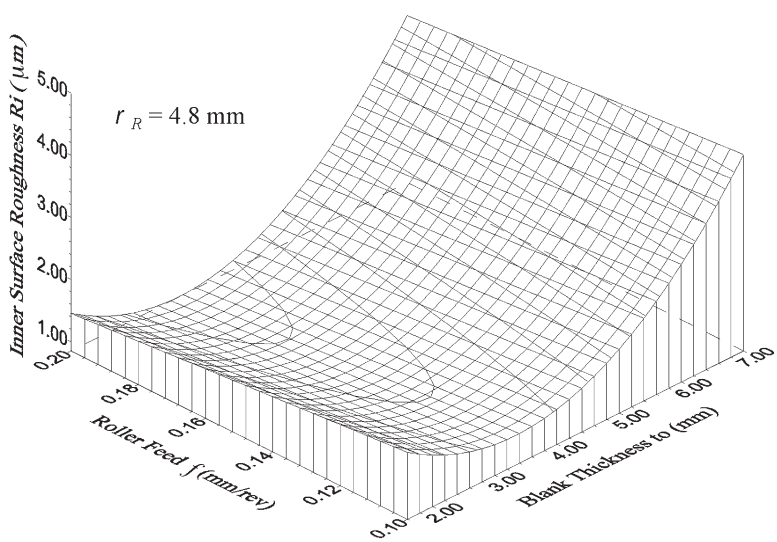

Fig. 9. Effects of blank thickness on the iner surface roughness at various roller feeds.

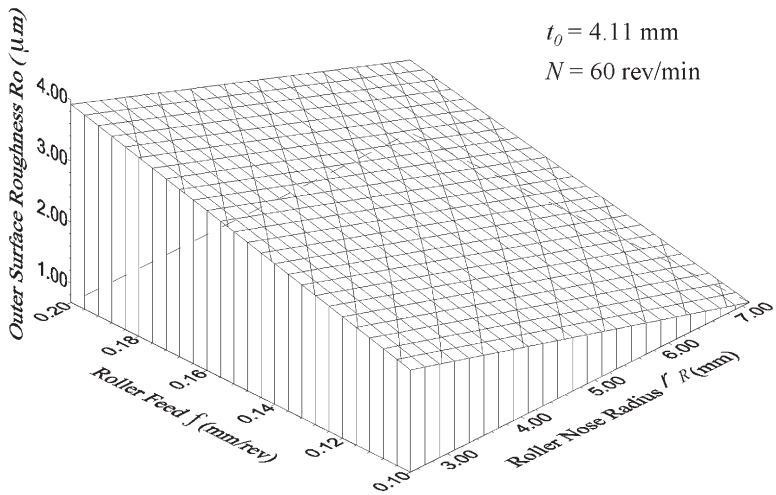

Fig. 10. Effects of roller nose radius on the outer surface roughness at various roller feeds.

$$\mathrm{Ft} = 800.25 - 4.36N + 0.04N^2 - 6323.02f - 0.27Nf + 21186f^2. \tag{3.8}$$

Fig. 11 illustrates the effects of mandrel revolutions on the tangential force at various roller feeds by applying Eq. (3.8). At a fixed mandrel revolution, the tangential force tends to decrease with a decreasing roller feeds and reaches a minimum force at roughly f=0.15 mm/rev. For roller feeds below this value, the tangential contact force grows. Conversely, at a fixed roller feed, the tangential contact force tends to decrease with increasing mandrel revolutions and then reaches a minimum at approx. N=55 rev/min. For mandrel revolutions greater than this value, the tangential

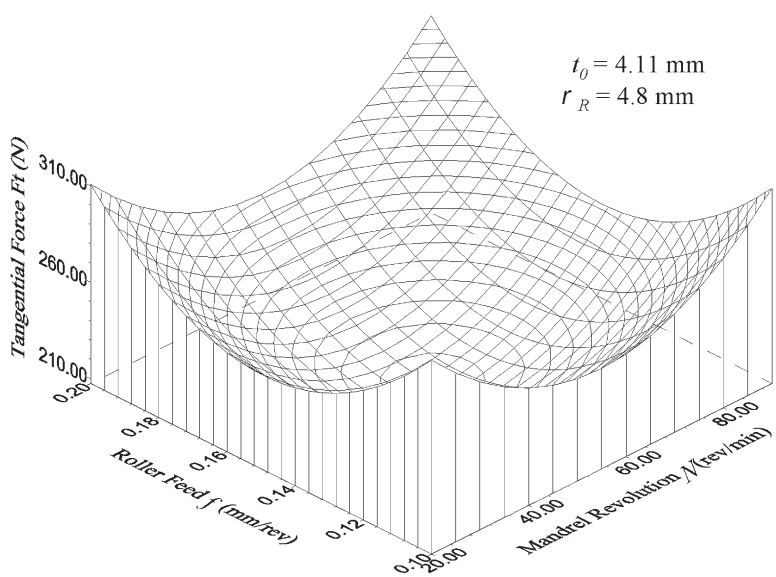

Fig. 11. Effects of mandrel revolutions on the tangential force at various roller feeds.

force expands again. The interactive effects of both the roller feeds and mandrel revolutions on the tangential force are evident. The least tangential force is reached at mandrel revolutions of approx. N=55 rev/min and a roller feeds of f=0.15 mm/rev.

For ρ_R=4.8 mm and f=0.16 mm/rev, Eq. (3.4) yields to:

$$Fp = 397.68 - 41.09t_0 + 11.74t_0^2 + 4.08N - 0.25t_0N - 0.03N^2. \quad (3.9)$$

Fig. 12 depicts the effects of blank thickness on the feeding force at various mandrel revolutions. At a fixed blank thickness, the feeding contact force tends to increase with the decreasing mandrel revolutions, then reaches a maximum at roughly N=60 rev/min. For mandrel revolutions smaller than this value, the feeding force decreases rapidly. In contrast, with a fixed mandrel revolution value, the feeding force increases with the increasing blank thickness. Of course, the thicker the blank, the more energy required for the material to deform. Obviously, the blank thickness has a substantial effect on the feeding force than the mandrel revolution does.

Substitute ρ_R=4.8 mm and f=0.16 mm/rev, Eq. (3.5) becomes:

$$Fq = 358.53 + 185.43t_0 - 12.29t_0^2 + 1.62N - 0.26t_0N - 0.01N^2. \quad (3.10)$$

Fig. 13 demonstrates Eqs. (3.10) as the effects of blank thickness on the normal force component at various mandrel revolutions. The finding verifies that regardless of the mandrel revolution, the normal force increases with the blank thickness. The blank thickness has an evident effect on the normal force. Therefore, a thicker blank requires greater energy to deform.

5. Conclusion

A shear spinning machine and special fixture were constructed to perform a series of shear spinning experiments. Cone shaped products were satisfactorily manufactured from sheet metal blanks with this machine. Regression equations for the shear spinning force and surface roughness

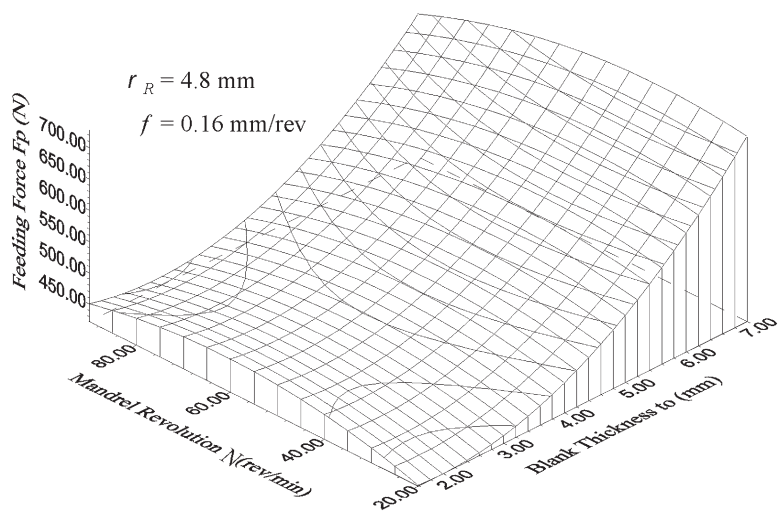

Fig. 12. Effects of blank thickness on the feeding force at various mandrel revolutions.

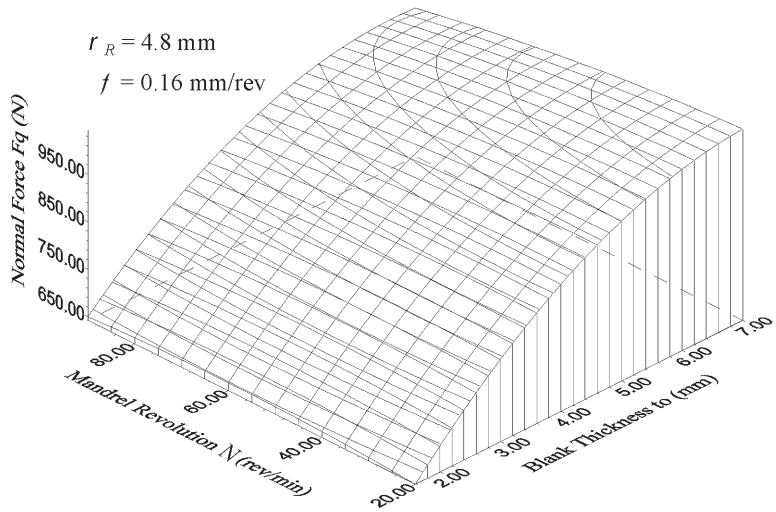

Fig. 13. Effects of blank thickness on the normal force at various mandrel revolutions.

of both inner and outer surface of the cone products were derived. Analytical data confirmed that the established regression equations were acceptable within 95% confidence level. Four additional independent experiments were performed for the purpose of verification with the regression equations. The experimental results corresponded with the established regression equations well. Therefore, it is concluded that the surface roughness and spinning force of the cone shaped products in shear spinning process can be determined with the proposed regression equations.

References

[1] S. Kobayashi, E.G. Thomsen, A theory of shear spinning of cones, Trans. ASME, Journal of Engineer for Industry 83 (1961) 485–495.
[2] H.C. Sortais, S. Kobayashi, E.G. Thomsen, Mechanics of conventional spinning, Trans. ASME, Journal of Engineer for Industry 85 (1963) 346–350.
[3] S. Kalpakcioglu, A study of shear spinnability of metals, Trans. ASME, Journal of Engineer for Industry 83 (1961) 478–484.
[4] S. Kalpakcioglu, Maximum reduction in power spinning of tubes, Trans. ASME, Journal of Engineer for Industry 86 (1964) 49–54.
[5] E. Siebel, K.A. Droge, Forces and material flow in spinning, Werkst attstechmk und Maschinenbau 45 (1) (1955) 6–9.
[6] J.N. Feola, Experimental analysis of shear deformation, M.S. thesis, Syracuse University, New York, 1955.
[7] M. Held, Determination of the material quality of copper shaped charge liners, Propellants, Explosives, Pyrotechnics 10 (1985) 125–128.
[8] Wang Delin, Cheng Xueliang, Wang Wei, Spinning forming technique and quality control of 30 CrMnSiA high precision end, Proceedings of the Fourth International Conference on Technology of Plasticity, China, 1993, pp. 1448–1452.
[9] G.E.P. Box, W.G. Hunter, J.S. Hunter, Statistics for Experiments: An Introduction to Design, Data Analysis and Model Building, Wiley, New York, 1978.
[10] D.C. Montgomery, Design and Analysis of Experiments, Wiley, New York, 1984.